Program Digest, 2019 IEEE International Ultrasonics Symposium (IUS)
Glasgow, Scotland, October 6-9, 2019

Linear prediction filtering of per channel data for noise reduction – theory of action and application to cardiac ultrasound

Francois Vignon[1], Junseob Shin[1], Jean-Luc Robert[1], Sheng-Wen Huang[1], Can Meral[1] , Iason Apostolakis[1], Man Nguyen[1], Roy Sivley[2], Fernando Quivira[2],
[1] *Philips Research North America, Cambridge, MA,* [2] *Philips Healthcare, Andover, MA, USA*
francois.vignon@philips.com

***Abstract* — Cardiac ultrasound imaging suffers from acoustic artefacts including diffraction limitation, aberration, reverberation, multipath, and electronic noise. In particular, multipath through the chest wall gives rise to a diffuse haze that obscures clinically relevant features.**

Linear prediction filtering applied to time-aligned array channel data has recently been introduced for white noise reduction in ultrasound. Our objectives in this work are 1) theoretical: to summarize the insights underpinning linear prediction filtering of array data thereby providing a mathematical framework to analyze its effects; and 2) experimental: to test the effectiveness of this technique in reducing multipath noise that produces diffuse cardiac haze.

A signal model of array data originating from a superposition of far-field point sources can be expressed with a fully deterministic recursion and interpreted as a linear prediction model. The linear prediction filter is the minimum mean square error estimator of the predictable signal components. Linear prediction filtering is equivalent to applying a spatial filter to the channel data prior to beam-sum. The filter, combined to beam-summing, is equivalent to a applying a post-filter (i.e. mask) to the beam-summed data, whose amplitude is the DC response of the filter.

Linear prediction filtering was applied on *in-vivo* cardiac datasets and compared to applying a Wiener postfilter designed to minimize the mean squared error of the beamformed output in the presence of white noise. Compared to Wiener filtering, the linear prediction filter was effective at reducing chamber haze levels, but it preserved sidelobe signals. The linear prediction framework may reduce scattering from structures of interest if the signal to interference ratio is low.

Keywords— Beamforming, Linear prediction filtering, noise reduction, multipath

I. INTRODUCTION

In cardiac imaging, multipath / multiple scattering from the chest wall and structures adjacent to the heart give rise to a haze that obscures the tissue and impedes diagnosis [1].

Linear prediction filtering is a commonly used technique for noise reduction [2]. The technique was recently introduced on ultrasound data where it was shown effective at eliminating white noise and its potential for eliminating multipath noise was expressed [3]. Linear prediction filtering assumes a signal model where the signal received at the array is the superposition of a finite sum of coherent wavefronts. Under such signal model, the signal of any array element can be predicted by the signal sensed at a finite number of neighboring array elements. The component that is not predicted corresponds to the residual noise, *i.e.* all that cannot be described by the signal model, including white noise and spatially broad-band multipath noise [3,4].

Applying linear prediction filtering to the array data prior to summing will therefore eliminate unpredictable signal components from the input data but will retain coherent on-axis and off-axis scattering events. Broadband white noise and multipath noise are largely eliminated, but sidelobe noise is preserved.

In the following we present the theory of linear prediction filtering applied to filtering broadband noise from per-channel data. We show that filtering and beamsummation is equivalent to applying a post-filter (mask) to the image, and compare this mask's properties to the Wiener post-filter [5], which was introduced to minimize noise in ultrasound images under pure white noise assumption. Finally, we test the effectiveness of the technique for removing cardiac haze *in vivo*.

II. THEORY

A. Signal model and recursion formula

The signal arriving at a 1D array, after time-delay compensation, is modeled as a discrete sum of a finite number of coherent scatterers. In the narrowband approximation, it writes:

$$s(n) = \sum_{i=1}^{p} \beta_i e^{jk_i n} \quad (1)$$

where p is the assumed number of scatterers and will also be referred to as *model order*, the β_i's are complex amplitudes (amplitude and phase) of the scattering events, the k_i's are spatial wavenumbers linked to the direction of arrival of the signal ($k_i = 2\pi \cdot pitch/\lambda \cdot \sin(\theta_i)$ where λ is the wavelength and θ_i the angular direction of arrival), and n indexes the array elements. $j = \sqrt{-1}$.

We will demonstrate that the signal can be modelled by a deterministic recursion, *i.e.* that the signal at channel n can be predicted by signals at p previous channels n-1 to n-p. The following is derived from [6].

Taking the Fourier transform along the array dimension (n):

$$S(k) = \sum_{i=1}^{p} \beta_i \delta(k - k_i) \tag{2}$$

where $\delta(\cdot)$ is the Kroenecker Delta function.

We can uniformly cancel $S(k)$ by multiplying it by a function that has zeroes at the k_i's, for example $P(k) = \prod_{i=1}^{p}\left(1 - e^{j(k-k_i)}\right)$:

$$P(k)S(k) = \prod_{i=1}^{p}\left(1 - e^{j(k-k_i)}\right) S(k) = 0 \tag{3}$$

$P(k)$ is a polynomial of degree p in e^{jk}. Let us write its expanded form as

$$P(k) = 1 - \sum_{i=1}^{p} a_i e^{jik} \tag{4}$$

where the a_i's result from the expansion and depend on the k_i's.

Replacing the expanded for of $P(k)$ in (3) we have

$$\left(\sum_{i=1}^{p} a_i e^{jik}\right) S(k) = S(k) \tag{5}$$

and, taking the inverse Fourier transform:

$$\left(\sum_{i=1}^{p} a_i \delta(n - i)\right) * \, s(n) = s(n) \tag{6}$$

where * is the convolution operator. Because $\delta(n - i) * s(n) = s(n - i)$ it comes

$$s(n) = \sum_{i=1}^{p} a_i s(n - i) \tag{7}$$

which is the recursion formula we were looking for and states that the signal at channel n can be predicted as a linear combination of its neighbors.

B. *Estimating the parameters of the recursion*

In practice, measurements are noisy, and we assume that the (noisy) channel $s(n)$ can only be predicted from its (noisy) neighbors up to a random error term $e(n)$, *i.e.*

$$s(n) = \sum_{i=1}^{p} a_i s(n - i) + e(n) \tag{8}$$

We can use a least squares minimization approach to estimate the a_i's given a model order. The a_i's are the ones that minimize the prediction mean squared error, i.e.

$$\{a_i\}_{i=1\ldots p} = argmin\ \mathrm{E}(|e(n)|^2)$$

$$= argmin\ \mathrm{E}\left(\left|s(n) - \sum_{i=1}^{p} a_i s(n - i)\right|^2\right) \tag{9}$$

where $\mathrm{E}(\cdot)$ denotes expected value. We can estimate the expected value by averaging over array index (n), i.e.

$$\{a_i\} = argmin\ \sum_{n=p+1}^{N}\left|s(n) - \sum_{i=1}^{p} a_i s(n - i)\right|^2 \tag{10}$$

This is the same as finding the minimum mean-squared error solution of the matrix equation

$$\mathbf{S} = \mathbf{\Sigma} \cdot \mathbf{A} \tag{11}$$

With $\mathbf{S} = [s(p + 1)\ s(p + 2) \ldots s(N)]^T$,
$\mathbf{A} = \left[a_1\ a_2 \ldots\ a_p\right]^T$, and

$$\mathbf{\Sigma} = \begin{bmatrix} s(p) & s(p-1) & \ldots & s(1) \\ s(p+1) & s(p) & \ldots & s(2) \\ \ldots & \ldots & \ldots & \ldots \\ s(N-1) & s(N-2) & \ldots & s(N-p) \end{bmatrix}$$

The least square error solution is

$$\mathbf{A} = (\mathbf{\Sigma}^H \mathbf{\Sigma})^{-1} \mathbf{\Sigma}^H \mathbf{S} \tag{12}$$

Once the a_i's are found through equation (11), they are used to predict each channel data from its neighbors according to

$$\hat{s}(n) = \sum_{i=1}^{p} a_i s(n - i) \tag{13}$$

$\hat{s}(n)$ is the linearly predicted channel data for element n, it is the estimate that minimizes the mean squared error between the predictable part of the signal according to the model, and the measured signal.

C. *Some remarks*

- *Forward-backward averaging:*

Note that in the above, channel n is predicted from its preceding neighbors (channels n-1 to n-p). We can also flip the array and predict channel n from its neighbors on the other side (channels n+1 to n+p); the final filtered signal is the average of the predicted signals in both directions, this is what is done in [3]. An alternative would be to predict channel n's signal from its neighbors on both sides. Analogous to eq. (7), we have

$$s(n) = \sum_{i=-\frac{p}{2}, i\neq 0}^{p/2} a_i s(n + i) \tag{14}$$

the derivation of the a_i's would proceed similarly as above.

- *Prediction filtering of per channel data and masking / post-filtering*

Once the predicted data $\hat{s}(n)$ is obtained, it is summed across the array to obtain the beamsummed data:

$$\hat{y} = \sum_{n=p+1}^{N} \hat{s}(n) = \sum_{n=p+1}^{N} \sum_{i=1}^{p} a_i s(n - i) \tag{15}$$

(we just inserted eq. (13) in the beamsum). Reverting the sums, it becomes

$$\hat{y} = \sum_{i=1}^{p} a_i \sum_{n=p+1}^{N} s(n - i) \tag{16}$$

If the model order is small compared to the total number of elements (p<<N), then $\sum_{n=p+1}^{N} s(n - i) \approx \sum_{n=1}^{N} s(n) = y$ (the beamsum of noisy data), as the difference is only in the contribution of a few edge elements. Therefore (16) simplifies:

$$\hat{y} \approx y \cdot \sum_{i=1}^{p} a_i \tag{17}$$

In other words, even though linear prediction filtering is understood and applied on the per-channel data, is can be applied equivalently as a complex post-filter (*i.e.* a mask) to the complex beam-summed data. The value of the mask, $\sum_{i=1}^{p} a_i$, is the D.C. response of the linear prediction filter. In other words, we are trading off some distortion to "desired signals" on-axis for white noise reduction since a distortionless response constraint would correspond to $\sum_{i=1}^{p} a_i = 1$.

- *Spectral estimation*

Starting from equation (8) that states that the residual between the true signal and its predicted value is a random noise term $e(n)$, *i.e.*

$$s(n) = \sum_{i=1}^{p} a_i s(n-i) + e(n) \quad (8)$$

we can take the Fourier transform of the above and obtain

$$S(k) \cdot \left(1 - \sum_{i=1}^{p} a_i e^{jik}\right) = E(k) \quad (18)$$

from which we deduce the power spectral estimate of the signal model:

$$E(|S(k)|^2) = \sigma_e{}^2 / \left(1 - \sum_{i=1}^{p} a_i e^{jik}\right) \quad (19)$$

and we see that the spatial frequencies / directions of arrival present in the signal model, i.e. the peaks of $E(|S(k)|^2)$, correspond to the zeroes of the polynomial $\left(1 - \sum_{i=1}^{p} a_i e^{jik}\right)$. Once these peaks $\{k_i\}_{i=1\ldots p}$ are found, the complex amplitudes $\{\beta_i\}_{i=1\ldots p}$ of the scatterers in the signal model of eq. (1) can be found by finding the β_i's that minimize the error between the signal model and the measured signal, *e.g.*

$$\{\beta_i\}_{i=1\ldots p} = argmin\ \mathrm{E}\left(\left|s(n) - \sum_{i=1}^{p} \beta_i e^{jk_i n}\right|^2\right) \quad (20)$$

The procedure described above is a known parametric spectral estimation technique called autoregressive modelling (AR) that applies to a signal comprised of peaks in random noise [6]. Once the signal model is known explicitly, it could be used to produce an image, estimate the noise, or both. This will be the object of further investigation; here we restrict ourselves to linear prediction filtering and its equivalent masking of equations (13), (15) and (17).

III. Methods

We first apply linear prediction filtering on a phantom dataset consisting of point scatterers. In this configuration, the signal model is valid, and the signal is completely preserved including the sidelobes (as long as the number of scatterers contributing to the per-channel data at any given location does not exceed the model order *p*). This is unlike other masking techniques such as the Wiener post-filter that attenuate sidelobes. Then, we apply the technique to *in vivo* cardiac datasets in parasternal long-axis and apical 4-chamber views.

We used a Philips S5-1 sector probe in fundamental mode. We filter the per-channel data around the band of interest with a quadrature band-pass filter. Then we apply the processing described in the previous section at each depth on the complex data, with a model order $p = 4$. Results are compared to applying the Wiener post-filter [5], which is a multiplicative mask W applied to the beam-summed data $y = \sum_{n=1}^{N} s(n)$. The Wiener mask is a more theoretically explicit trade off between signal and noise attenuation as it is designed to minimize the mean-squared error between the true (noiseless) beam-summed signal x and the weighted noisy beam-summed signal y as

$$W = argmin\ E(|x - W \cdot y|^2) \quad (21)$$

Under the assumption that true signal and noise are decorrelated, the solution to (21) is

$$W = E(|x|^2) / (E(|x|^2) + E(|y - x|^2)) \quad (22)$$

In this paper we follow the approximations in [5] which define W from the measured per-channel data as

$$W = |y|^2 / (|y|^2 + \sigma^2) \quad (23)$$

where σ^2 is an estimate of the beamformed noise power assuming white channel noise:

$$\sigma^2 = \sum_{n=1}^{N} |s(n) - y/N|^2 \quad (24)$$

IV. Results

All results are presented on the following page (1: point scatterer simulation; 2: apical 4-chamber view, 3: parasternal long-axis view), showing: top row, from left to right: the default Delay-and-Sum image | with linear prediction filtering of per channel data | with Wiener post-filtering; Bottom row, from left to right: the equivalent post-filter for linear prediction filtering | the Wiener post-filter. Images are shown with equal gain and a 70dB dynamic range, masks are shown on a [0 1] scale.

Upon quantitative analysis, linear prediction filtering of cardiac data significantly improved endocardium-to-chamber contrast (*e.g.* from 17 to 24 dB in the apical 4-chamber view) but the contrast-to-noise ratio was unchanged.

Compared to Wiener filtering, the linear prediction filter was effective at reducing chamber haze levels but preserved sidelobe artefacts, as expected.

V. Discussion

Although the results are encouraging with reduced cardiac haze and preserved endocardium, the evidence is insufficient to conclude on clinical usefulness. Further validation work should include implementation on harmonic imaging, which is the default mode in clinical echocardiography, and testing on more datasets in a varied patient population and a variety of views.

Further design work should focus on a better implementation matching the theory with clinical reality. For example, here we compute the linear prediction coefficients from complex broadband data from the entire array, but 1) the theory is narrowband, and 2) in general, signals will not be stationary across the array, due to both the broadband nature of the signal and the heterogeneity of the acoustic window (*i.e.* partial array blockage) and the propagation path. Note that a broadband implementation was provided in [3].

Finally, linear prediction filtering does not guarantee to preserve the on-axis signal if the signal to noise ratio is low: if the signal of interest is not one of the *p* strongest components in the per-channel data, the algorithm will reject it. A successful algorithm will need a safeguard against this situation.

References

[1] A. Fatemi, E.A. Rye Berg, and A. Rodriguez Molares, “Studying the origin of reverberation clutter in echocardiography: *in vitro* experiemnts and *in vivo* demonstrations”, Ultrasound in Med. & Biol. 45 (7), July 2019

[2] P.P. Vaidyanathan, “The theory of linear prediction”, Synthesis lectures on signal processing #3, Morgan and Claypool, publishers.

[3] J. Shin and L. Huang, “Spatial Prediction Filtering of Acoustic Clutter and Random Noise in Medical Ultrasound Imaging”, IEEE Trans. Med. Im. 36(2), February 2017.

[4] A. Aubry and A. Derode, “Multiple scattering of ultrasound in weakly inhomogeneous media: Application to human soft tissues”, J. Acoust. Soc. Am. 129 (225), 2011

[5] C.I. Nilsen and S. Holm, “Wiener Beamforming and the Coherence Factor in Ultrasound Imaging”, IEEE TUFFC 57 (6), June 2010

[6] P. Stoica and R. Moses, “Spectral analysis of signals”, ch. 4: Parametric Models for Line Spectra, Prentice Hall, Ed.

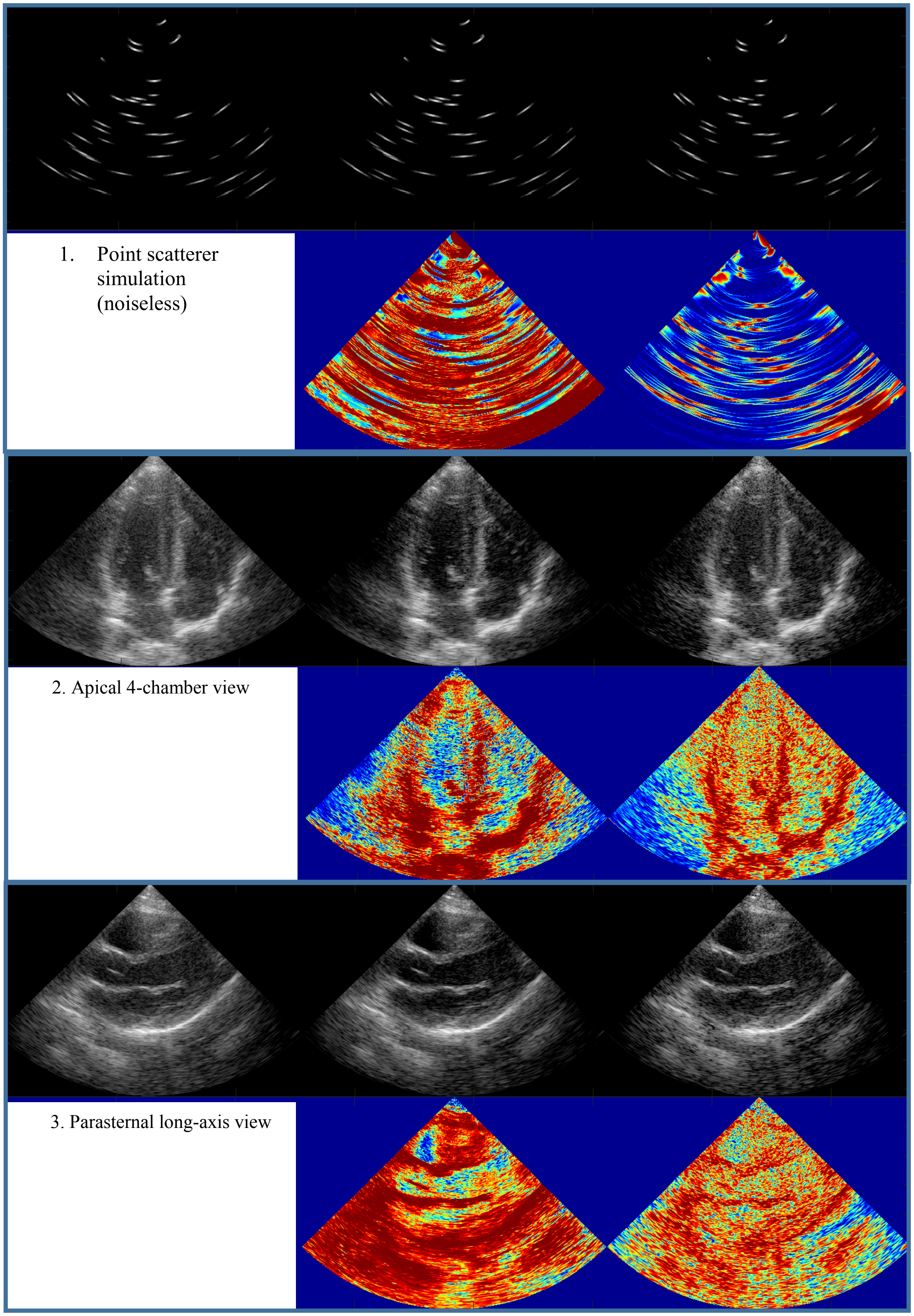
1. Point scatterer simulation (noiseless)
2. Apical 4-chamber view
3. Parasternal long-axis view